

70-47-TM  
047 251

SATELLITE ANALYSES OF CIRRUS CLOUD PROPERTIES  
DURING THE FIRE PHASE-II CIRRUS INTENSIVE FIELD OBSERVATIONS  
OVER KANSAS

Patrick Minnis<sup>1</sup>, David F. Young<sup>2</sup>, Patrick W. Heck<sup>2</sup>, Kuo-Nan Liou<sup>3</sup>, and  
Yoshihide Takano<sup>3</sup>

<sup>1</sup>NASA Langley Research Center, Hampton, VA, USA 23665-5225

<sup>2</sup>Lockheed Engineering and Sciences Co., Hampton, VA, USA 23666

<sup>3</sup>University of Utah, Salt Lake City, UT, USA 82101

Presented at

11th International Conference on Clouds and Precipitation  
Montreal, Canada  
August 17-21, 1992

# SATELLITE ANALYSES OF CIRRUS CLOUD PROPERTIES DURING THE FIRE PHASE-II CIRRUS INTENSIVE FIELD OBSERVATIONS OVER KANSAS

Patrick Minnis<sup>1</sup>, David F. Young<sup>2</sup>, Patrick W. Heck<sup>2</sup>, Kuo-Nan Liou<sup>3</sup>, and Yoshihide Takano<sup>3</sup>

<sup>1</sup>NASA Langley Research Center, Hampton, VA, USA 23665-5225

<sup>2</sup>Lockheed Engineering and Sciences Co., Hampton, VA, USA 23666

<sup>3</sup>University of Utah, Salt Lake City, UT, USA 82101

## 1. INTRODUCTION

The First ISCCP (International Satellite Cloud Climatology Project) Regional Experiment (FIRE) Phase II Intensive Field Observations (IFO) were taken over southeastern Kansas between November 13 and December 7, 1991, to determine cirrus cloud properties. The observations include in situ microphysical data; surface, aircraft, and satellite remote sensing; and measurements of divergence over meso- and smaller-scale areas using wind profilers. Satellite remote sensing of cloud characteristics is an essential aspect for understanding and predicting the role of clouds in climate variations. The objectives of the satellite cloud analysis during FIRE are to validate cloud property retrievals, develop advanced methods for extracting cloud information from satellite-measured radiances, and provide multiscale cloud data for cloud process studies and for verification of cloud generation models. This paper presents the initial results of cloud property analyses during FIRE-II using Geostationary Operational Environmental Satellite (GOES) data and NOAA Advanced Very High Resolution Radiometer (AVHRR) radiances.

## 2. DATA

GOES visible (VIS, 0.65  $\mu\text{m}$ ) data taken every half hour at the nominal 1-km resolution were averaged to obtain an effective 4-km resolution to match the corresponding 4-km x 8-km infrared window (IR, 11.2  $\mu\text{m}$ ) radiances. Each scan line of the IR data was duplicated to achieve an effective 4-km resolution. Radiances at 12.7  $\mu\text{m}$  (channel 7) were also taken each half hour at a 14-km resolution using the GOES multispectral imager (MSI). Data from the MSI channel 12 (3.94  $\mu\text{m}$ ) were taken with the VIS, IR and channel 7 radiances at 20 minutes after the hour at 3-hour intervals. The MSI data were duplicated to obtain the same resolution as the IR data. AVHRR channels 1 (0.67  $\mu\text{m}$ , VIS), 3 (3.73  $\mu\text{m}$ ), 4 (10.8  $\mu\text{m}$ , IR), and 5 (12.0  $\mu\text{m}$ ) were also taken at a 1-km resolution from the NOAA-11 and NOAA-12. These satellites have ascending nodes at 1430 and 0730 local time (LT), respectively.

In addition to standard 12-hourly soundings at the National Weather Service (NWS) stations, temperature and humidity profiles were taken from hourly Cross-Chain Loran Atmospheric Sounding System (CLASS) soundings at several sites in the vicinity of Coffeyville, KS, the hub of the experiment (Fig. 1). Cloud-top heights were derived from lidar backscattering profiles. Surface lidars were located at the hub; Parsons, KS; and in northeastern Oklahoma. A down-looking lidar was flown on the NASA ER-2 at various times during FIRE-II.

## 3. METHODOLOGY

### a. Visible and infrared retrievals

During the daytime, cloud amount and height are derived with several techniques. One method uses the VIS and IR channels in a manner similar to that used to analyze the ISCCP data. The VIS reflectance,  $\rho_v$ , is interpreted with a parameterization of radiative transfer calculations using the scattering characteristics of a specified particle size distribution.

Only two distributions are considered here, a water-droplet distribution having an effective radius of 10  $\mu\text{m}$  and an effective variance of 0.05, and a cirrostratus (CS) hexagonal ice-crystal distribution (Takano and Liou, 1989). The water-droplet (WD) distribution, close to that used by the ISCCP, was used to compute a Mie-scattering phase function. The CS phase function was derived from ray tracing. An optical depth,  $\tau_v$ , is derived with the parameterization from a given reflectance observation using one of the two models. In addition to the cloud reflectance, the parameterization accounts for the surface reflectance, Rayleigh scattering, and ozone absorption. The VIS optical depth is then used to compute IR emissivity of the cirrus cloud which is then used to correct the observed equivalent blackbody temperature,  $T_{IR}$ , to obtain a better estimate of the true radiating temperature of the cloud,  $T_c$ . The value of  $T_c$  is then converted to cloud height,  $z_c$ , using the nearest available sounding. Estimates of the clear-sky temperature,  $T_s$ , and clear-sky reflectance,  $\rho_{vs}$ , are needed to perform this analysis. The clear-sky reflectance map was developed from minimum reflectances taken during November 1986. Clear-sky temperature was derived as described by Minnis et al. (1987). Details of the technique, the parameterizations, and the models are given by Minnis (1991).

For intercomparison with the surface and aircraft data, only data within a small area around the sensor are extracted from the image. To provide a larger scale cloud-parameter dataset for model intercomparison, the data are analyzed half-hourly on a 0.5° grid covering the area between 32°N and 42°N and between 93°W and 103°W. The VIS and IR data are converted to two-dimensional histograms following the methods of Minnis et al. (1990).

### b. Multispectral infrared retrievals

Another technique applicable both day and night uses

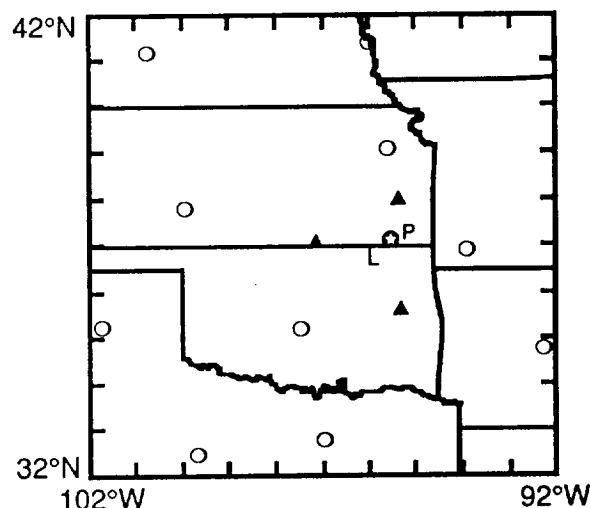


Fig. 1. Locations of Coffeyville (O), Parsons (P), University of Wisconsin lidar (L), NWS sites (O), and CLASS sites (▲).

brightness temperature differences that arise from variations of cloud optical properties with wavelength and the nonlinearity of the Planck function with wavelength. Estimates of cloud emissivity, cloud height, and cloud microphysics can be derived theoretically from an analysis of multispectral infrared data [IR channels 7 and 12 (GOES) or channels 3, 4, and 5 (AVHRR)] by taking advantage of the observed temperature differences. These differences have been examined both theoretically and with observations in attempts to derive various cloud properties from the satellite data (e.g., Allen et al., 1990; Stone et al., 1990; Parol et al., 1991). As in the earlier methods, the technique used here attempts to find the best match between the observations and theoretical calculations.

Radiative transfer calculations using an adding doubling model were performed for a range of particle sizes and shapes. Cirrus clouds were modeled using ice spheres with effective radii,  $r = 4, 8, 16, 32$ , and  $64 \mu\text{m}$ , and hexagonal crystals having the CS and cirrus uncinus (CU) distributions (Takano and Liou, 1989). Surface temperatures,  $T_g$ , were varied from 260 K to 320 K. Cloud temperatures ranged from 210 K to 270 K. Atmospheric attenuation of the IR radiances was estimated in the same manner used by Minnis (1991). The channel-7 and -12 atmospheric absorption optical depths were 2 and 0.75 times the corresponding IR values, respectively. The channel-3 and -5 optical depths were set at 1.25 and 0.75 times the channel-4 values, respectively. The computations were performed for both a wet and dry atmosphere.

The results were parameterized as

$$\epsilon_i = \sum_{n=0}^3 a_n \ln(\tau_v / \mu)^n + a_4 \ln(\Delta T_{SC}) + a_5 \mu, \quad (1)$$

where  $\epsilon_i$  is the effective emittance for channel  $i$ ,  $\Delta T_{SC} = T_s - T_c$ , and  $\mu = \cos\theta$ , and  $\theta$  is the satellite zenith angle. Two sets of coefficients,  $a_i$ , were determined for each channel, one for  $\Delta T_{SC} \geq 5\text{K}$  and another for  $\Delta T_{SC} < 5\text{K}$ . The effective emittance includes both the absorption and scattering effects of the cloud. The parameterization fits the radiative transfer results with an rms error of  $\pm 0.02$  and  $\pm 0.03$  for large and small  $\Delta T_{SC}$ 's, respectively. The VIS optical depth is  $\tau_v = Q_{exv} \tau_i / Q_{exl}$ , where  $Q_{ex}$  is the extinction efficiency and  $\tau_i$  is the extinction optical depth for channel  $i$ .

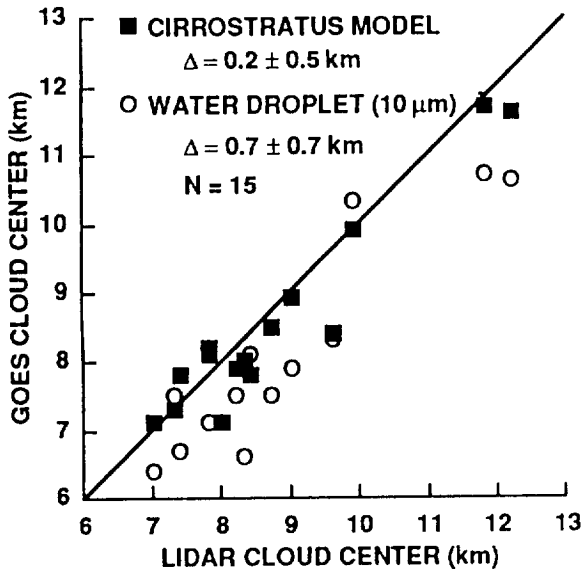


Fig. 2. Comparison of surface lidar and satellite-derived cloud-center heights over Parsons, KS.

A given radiance observation is modeled as

$$B_i(T) = (1 - C) B_i(T_{si}) + C[\epsilon_i B_i(T_c) + (1 - \epsilon_i) B_i(T_{si})], \quad (2)$$

where  $B_i$  is the Planck function at the center of channel  $i$  and  $C$  is the cloud fraction.

Similarly, calculations were performed for solar reflectance in the VIS and GOES channel 12 for the CS and CU distributions and for Mie-scattering water droplet distributions having an effective variance of 0.1 and  $r = 2, 4, 6, 8, 12, 16, 32$ , and  $64 \mu\text{m}$ . The results were used to develop a set of bidirectional reflectance models,  $\rho_i(k_i, \tau_i, \theta_o, \theta, \psi)$ , where  $k_i$  is the microphysical model,  $\theta_o$  is the solar zenith angle, and  $\psi$  is the relative azimuth angle. Thus, in the daytime, for channels 12 (GOES) or 3 (AVHRR), the observed radiance is approximated as

$$B_i(T) = B_i(T) + \mu_o E_i [\rho_i C + (1 - C) \rho_{si}], \quad (3)$$

where  $\mu_o = \cos\theta_o$ ,  $E_i$  is the solar constant at the central wavelength of channel  $i$ , and  $\rho_{si}$  is the clear-sky reflectance for channel  $i$ . Values for  $\rho_{si}$  are estimated at 0.05 and 0.10 over land and water, respectively. The non-unit emittance of these surfaces is included in the clear-sky measurements of  $T_s$  at night. The separate modeling of the emission and reflectance for these channels accounts for the diffuse surface source and the beam solar source.

## 4. RESULTS

### a. Preliminary VIS-IR results

An initial comparison of weighted cloud-center heights from the NASA Langley lidar (J. M. Alvarez, personal communication) with the cloud heights derived using VIS and IR GOES data over a small area surrounding Parsons, KS, is shown in Fig. 2. These data were taken at various times during FIRE-II. As in Minnis (1991), the CS model produces cloud center heights which are within 0.2 km of the lidar-derived values. The WD model yields underestimates of the cloud heights. Additional data covering more hours and sites are being analyzed.

The prime case study day for FIRE-II is November 26, 1991. During this day, thin cirrus replaced clear skies over the hub around noon and produced a halo around the Sun. A broken cirrus layer had developed around 2000 UTC (Universal Time Coordinated) centered near 9 km. The surface lidars also indicated a lower deck at 6.5 km with multiple levels reported by surface observers to the north and west. Multilayered clouds prevailed with a low-level cloud deck moving in from the south. Both a large-scale network and an inner network of frequent (3-6 hr) rawinsonde launches and extensive wind profiler, aircraft, and surface measurements provide an exceptional dataset for defining and monitoring the dynamics of this developing cyclone over the south-central Great Plains.

Figures 3 and 4 show sequences of cloud height and optical depth, respectively, resulting from the gridded analyses for four times during November 26. A clear zone around the hub at 1600 UTC filled in by 1900 UTC and remained overcast through 2100 UTC. High clouds predominate over Kansas and Oklahoma at 1600 UTC followed by a mix of cloud layers which give rise to the lower cloud heights during the afternoon. Low clouds ( $z_c \leq 2\text{ km}$ ), evident over north Texas in the morning, spread northward during the day. They are probably obscured by the higher clouds over southeastern Kansas. Thin cirrus clouds ( $\tau_v < 4$ ;  $z_c > 7\text{ km}$ ) are seen over part of eastern Kansas and much of Oklahoma at 1600 UTC while denser, high-level clouds are found over northern and central Kansas. By 1900 UTC, the thin cirrus clouds are mainly over southeastern Kansas with average cloud top heights over 7 km. At 2030 UTC, thin cirrus clouds with mean heights over 9 km pervade over eastern Kansas, Missouri, and central Arkansas.

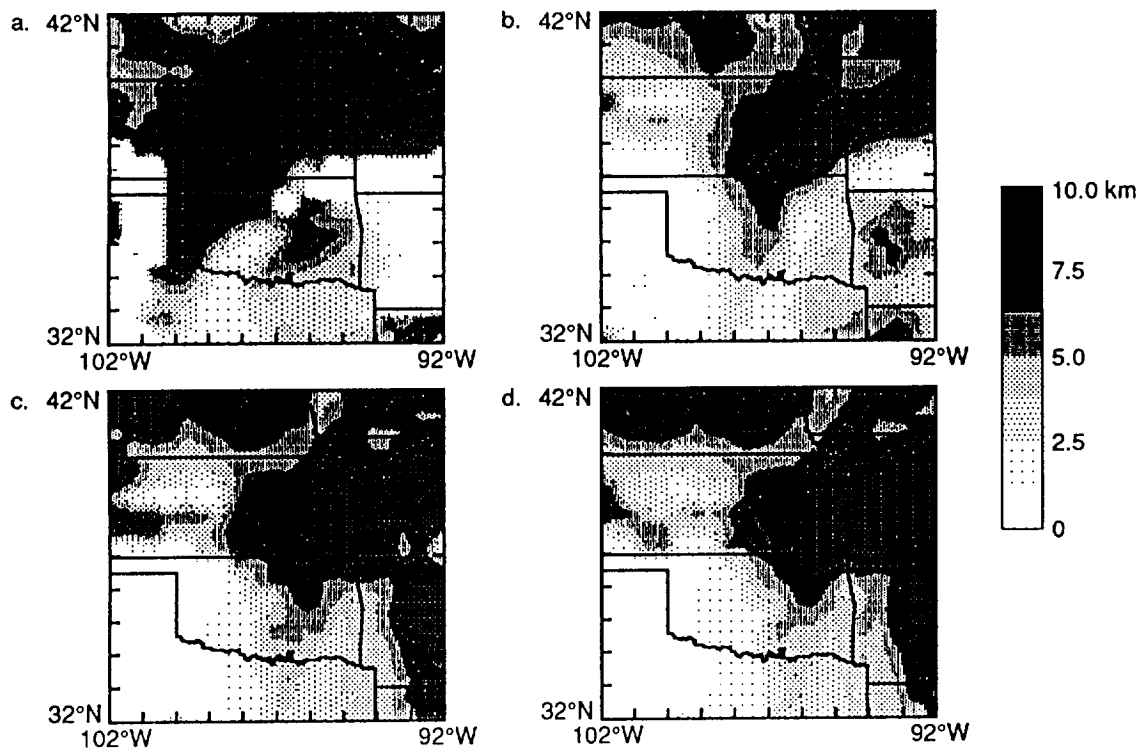


Fig. 3. GOES-derived cloud-center height (km) from November 26, 1991 at a) 1600 UTC, b) 1900 UTC, c) 2030 UTC, and d) 2100 UTC.

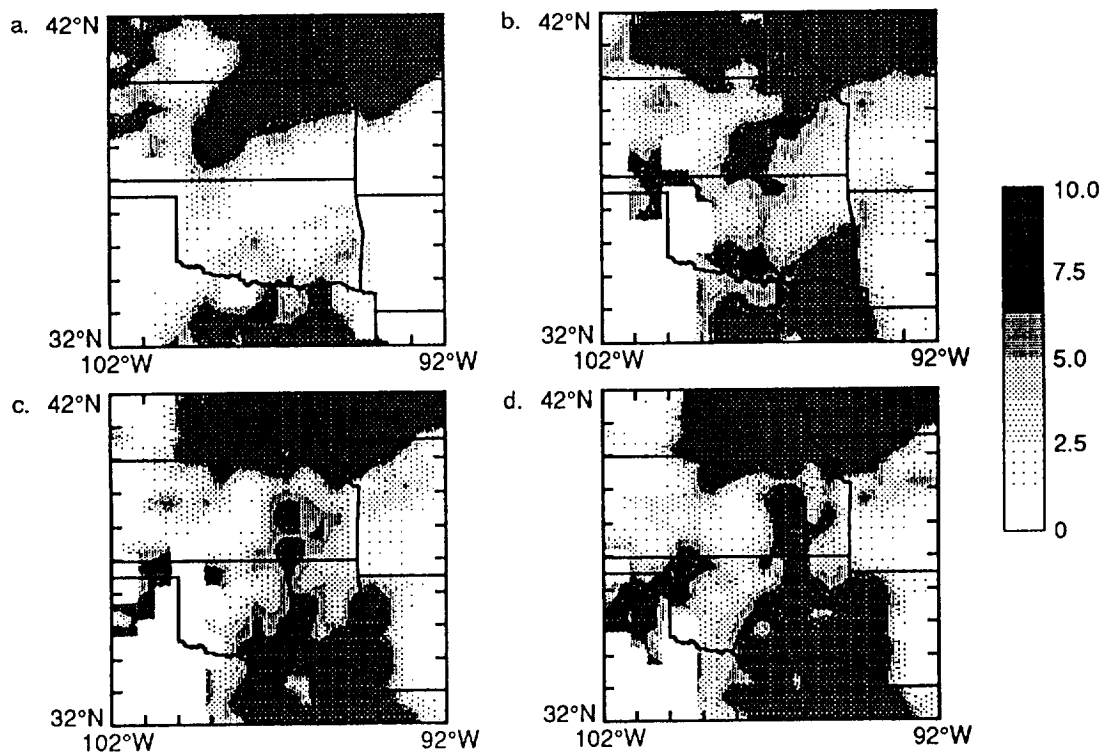


Fig. 4. GOES-derived visible optical depth from November 26, 1991 at a) 1600 UTC, b) 1900 UTC, c) 2030 UTC, and d) 2100 UTC.

These preliminary satellite analyses produce results that qualitatively agree with the observers' notes and quantitatively match the surface lidar reports. Figures 3 and 4 depict just a few of the products which are derived on a half-hourly basis from GOES VIS-IR data. Since the gridded analyses yield values for parameters that can be produced with mesoscale or larger scale models, they will be also useful for model development and validation. Therefore, such results should greatly enhance our capability to understand the complex dynamics and energetics involved in the development and dissipation of cirrus clouds.

#### b. Preliminary IR multispectral results

Cirrus was observed during the night of December 5, 1991 over Coffeyville, KS at  $\sim 9$  km (K. Sassen, personal communication) which corresponds to a temperature of 234 K. Figure 5 shows a histogram of temperature differences between channel 7 and 12 from the GOES versus the channel-7 brightness temperatures. The heavy dark lines delineate the variation of these differences with  $\tau_v$  and C computed with the parameterizations for an ice-sphere distribution having  $r = 16 \mu\text{m}$ . Assuming that the cirrus particles had this distribution, this plot indicates that most of the clouds passing over the lidar site were thin ( $\tau_v < 3$ ) and broken ( $C \sim 50\%$ ). Overall, this model encompasses these data better than those for the larger and smaller effective radii. Using a third channel, it should be possible to determine particle size, cloud temperature, and cloud fraction without the aid of the surface data.

#### 5. CONCLUDING REMARKS

Initial results from studying cirrus clouds using multispectral GOES data have been presented. Other comparisons using simultaneous GOES and AVHRR data are in progress. The cloud parameters that can be derived using these datasets will be used in process studies of cirrus clouds and validation of modeling efforts.

#### REFERENCES

- Allen, Jr., P. A. Durkee, and C. H. Wash, 1990: Snow/Cloud discrimination with multispectral satellite measurements. *J. Appl. Meteorol.*, **29**, 994-1004.
- Minnis, P., 1991: Inference of cirrus cloud properties from satellite-observed visible and infrared radiances. PhD dissertation, University of Utah, Salt Lake City, 161 pp.
- Minnis, P., E. F. Harrison and G. G. Gibson, 1987: Cloud cover over the eastern equatorial Pacific derived from July 1983 ISCCP data using a hybrid bispectral threshold method. *J. Geophys. Res.*, **92**, 4051-4073.
- Minnis, P., P. W. Heck, and E. F. Harrison, 1990: The 27-28 October 1986 FIRE IFO Cirrus Case Study: Cloud parameter fields derived from satellite and lidar data. *Mon. Wea. Rev.*, **118**, 2426-2446.
- Parol, F., J. C. Buriez, G. Brogniez, and Y. Fouquart, 1991: Information content of AVHRR channels 4 and 5 with respect to the effective radius of cirrus cloud particles. *J. Appl. Meteorol.*, **30**, 973-984.
- Stone, R. S., G. L. Stephens, C. M. R. Platt, and S. Banks, 1990: The remote sensing of thin cirrus cloud using satellites, lidar, and radiative transfer theory. *J. Appl. Meteorol.*, **29**, 353-366.
- Takano, Y. and K. N. Liou, 1989: Radiative transfer in cirrus clouds: I. Single scattering and optical properties of oriented hexagonal ice crystals. *J. Atmos. Sci.*, **46**, 3-19.

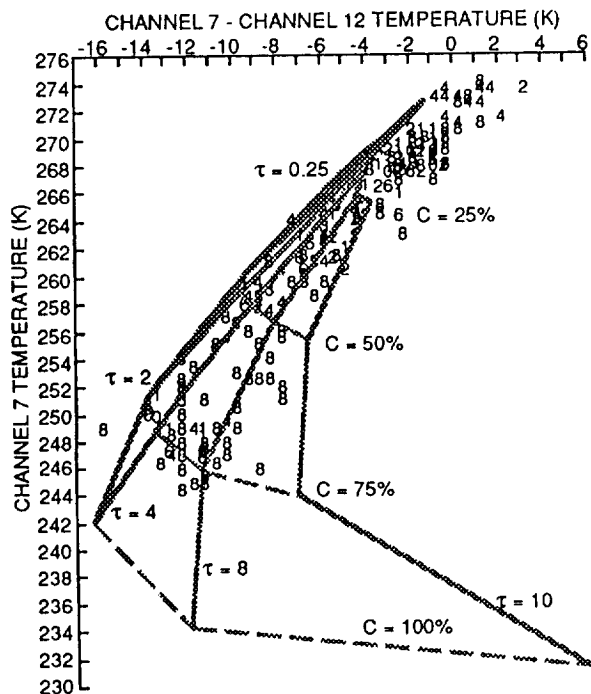


Fig 5. IR multispectral histogram for data over Coffeyville at 0920 UTC on December 5, 1991. The heavy lines represent model results for effective ice particle radius of  $16 \mu\text{m}$ .